Published in final edited form as:
Bone. 2010 March ; 46(3): 820–826. doi:10.1016/j.bone.2009.10.037.

CRTAP deficiency leads to abnormally high bone matrix mineralization in a murine model and in children with Osteogenesis Imperfecta type VII

N Fratzl-Zelman[1], **R. Morello**[2,*], **B Lee**[2,3], **F Rauch**[4], **FH Glorieux**[4], **BM Misof**[1], **K Klaushofer**[1], and **P Roschger**[1]

[1]Ludwig Boltzmann Institute of Osteology at Hanusch Hospital of WGKK and AUVA Trauma Centre Meidling, 4th Med. Dept. Hanusch Hospital, Vienna, Austria

[2]Department of Molecular and Human Genetics, Baylor College of Medicine, Houston, TX, USA

[3]Howard Hughes Medical Institute, Houston, TX, USA

[4]Genetics Unit, Shriners Hospital for Children, Montreal, Canada

Abstract

Cartilage-associated protein (CRTAP) is an essential cofactor for the proper post-translational chain modification and collagen folding. *CRTAP* mutations lead in mice (*Crtap*−/− mice) and humans (OI type VII) to a severe/lethal osteochondrodystrophy; patients have fractures at birth, deformities of the lower extremities and impaired growth. The consequences of CRTAP deficiency on intrinsic bone material properties are still unknown. In the present study we evaluated bone quality based on quantitative backscattered electron imaging (qBEI) to assess bone mineralization density distribution (BMDD) in femurs from 12 weeks old *Crtap*−/− mice and transiliac bone biopsies from 4 children with hypomorphic mutations and having residual CRTAP expression.

The analyses revealed in the bone matrix of *Crtap*−/− animals and OI type VII patients a significant increase in mean (CaMean) and most frequent mineral concentration (CaPeak) compared to wild-type littermates and control children, respectively. The heterogeneity of mineralization (CaWidth) was reduced in *Crtap*−/− mice but normal in OI type VII patients. The fraction of highly mineralized bone matrix (CaHigh) was remarkably increased in the patients: cancellous bone from 2.1 to 3.7 times and cortical bone from 7.6 to 25.5 times, associated with an increased persistence of primary bone. In conclusion, the BMDD data show that CRTAP deficiency results in a shift towards higher mineral content of the bone matrix similar to classical OI with collagen gene mutations. Our data further suggest altered mineralization kinetics resulting ultimately in an overall elevated tissue mineralization density. Finally, in OI type VII patients the increased portion of primary bone is most likely reflecting a disturbed bone development.

Keywords

CRTAP deficiency; Bone mineralization density distribution (BMDD); Quantitative backscattered electron imaging (qBEI); mouse femur; bone biopsy

Corresponding author: Dr. Nadja Fratzl-Zelman Ph.D, Ludwig Boltzmann Institute of Osteology, UKH Meidling, Kundratstrasse 37, A-1120 Vienna, Austria. Tel: +43-(0)1-60150-2652, Fax: +43-(0)1-60150-2651. nadja.fratzl-zelman@osteologie.at.
*Current address: Dept. of Physiology & Biophysics, University of Arkansas for Medical Sciences, Little Rock, AR 72205

Introduction

Cartilage-associated protein (CRTAP) is a component of the collagen prolyl 3-hydroxylation complex, a newly described post-translational modification system, which plays a critical role for the proper collagen helix formation in the cell [1,2]. This ER complex, which involves a prolyl 3-hydroxylase-1 (P3H1) enzyme, CRTAP and cyclophilin B, a peptidyl prolyl cis-trans isomerase, is responsible for the modification of a single proline residue (Pro 986) on each α1 (I) collagen chain into a 3-hydroxyproline (3-Hyp) [1]. Most interestingly, lack of CRTAP in vivo results in a loss of function of the prolyl 3–hydroxylation complex and an over-modification of the collagen helix at multiple residues by ER resident lysyl- and prolyl 4-hydroxylases [2,3].

The physiological importance of a functional prolyl 3-hydroxylation complex for normal bone formation is highlighted by the fact that deficiency of CRTAP or P3H1 cause a very severe to lethal bone dysplasia in mice and children [2,4–7]. *Crtap*−/− mice develop progressive and severe kyphoscoliosis over the first six months of age exhibiting pre- and postnatal growth delay with shortening of the proximal limb bones and osteopenia [5]. Moreover, bone histomorphometry has revealed decreased osteoid deposition and bone formation rate as well as decreased mineralization apposition rate and mineralization lag time in spite of normal osteoblast number [5]. Patients with null defects in CRTAP almost invariably die in the perinatal period [4,7], whereas those with hypomorphic mutations, i.e. having still residual CRTAP expression, survive. However, they have fractures at birth, deformities of the lower extremities and impaired growth [2,5]. Histomorphometric parameters in these patients revealed reduction in bone volume, elevated bone turnover and a decreased net bone formation rate, which represent striking similarities with moderately deforming to severe osteogenesis imperfecta (OI) [5].

Traditionally, OI has been described as a heterogeneous genetic syndrome with dominant inheritance characterized by low bone mass and high bone fragility caused by mutations in *COL1A1* or *COL1A2*, the two genes encoding the α chains of type I collagen [8,9]. Initially, four clinical phenotypes were distinguished reflecting disease severity [8,9]. OI bone is brittle in mouse models and humans due to higher mineral content, reduced collagen properties and altered bone nanostructure [10–17]. We have recently reported similarly increased mean mineral content in severe (OI type III and IV) and moderate OI (type I) [18,19]. Importantly, and most unexpectedly, we found the same increased mineralization density in patients having either a decreased amount of structurally normal collagen (OI type I with quantitative mutation) or structurally altered collagen (OI type I with qualitative mutation). This suggests that the increase in mineral content in bone tissue might not be caused by the impaired collagen structure itself [19].

The four new, non “classical” forms of OI that have been characterized more recently, share in common clinical and radiological criteria of “classical” OI but lack mutations in the collagen genes [20–22]. In contrast to OI types V and VI with still unknown etiology, recessive OI type VII and OI type VIII have been recently linked to CRTAP and P3H1 deficiency, respectively [2,4–6]. Moreover, the phenotype of *Crtap*−/− mice mimics well that of surviving patients with OI type VII carrying a quantitative defect in CRTAP expression [5]. Thus, it would be clinically interesting to explore the effect of CRTAP deficiency on bone material properties in comparison to OI forms with collagen gene mutations.

In the present study, we analyzed by quantitative backscattered electron imaging (qBEI) the bone mineralization density distribution (BMDD) in femurs from *Crtap* deficient mice as well as in trabecular and cortical bone from transiliac biopsy samples of four children with recessive OI type VII and about 10% residual CRTAP expression [5,22]. We further compared BMDD-

parameters of trabecular bone from these patients with our previously published data of OI types I, III and IV) [18,19].

Material and Methods

Animals

Femora were harvested from 12 week-old *Crtap*+/+ (n=15) and *Crtap*−/− mice (n=12) (males and females were pooled). The Crtap mouse colony was maintained in a mixed 129Sv/ev-C57Black/6J genetic background and housed in the Baylor College of Medicine Animal Vivarium under supervision of trained veterinarians according to standard conditions of the Center of Comparative Medicine under provisions of all applicable federal and state guidelines.

Subjects

The study group comprised four girls with OI type VII who are followed at the Shriners Hospital for Children in Montreal, Canada. All subjects are related (three sisters and their first cousin). The clinical and histomorphometric characteristics of these patients have been described in detail before (patients V-3, V5, V-6 and V-7 from the Ward et al., pedigree) [22] The diagnosis of OI VII was made on the basis of clinical, radiological and histological features of the disease and confirmed by mutation analysis of the *Crtap* genes [5]. The mutation shared by the four children is: c.472–1021C>G in intron 1 of the CRTAP gene. Two of the children (patients V-3 and V-7 from the Ward et al., pedigree) [22] had their CRTAP expression levels measured, and Q-PCR analysis demonstrated levels of CRTAP mRNA to be about 10% those of controls, as shown in Figure 6D in Morello et al, 2006 [5].

None of these children had received pharmacological treatment other than vitamin and calcium supplementation prior to the iliac crest bone biopsy. Samples were obtained between 2.3 and 8.5 years of age. Two bone samples were available from patient V-3 at 2.3 and 4.2 years and three samples from patient V-5 at 2.7, 4.7 and 8.5 years. Patients V-6 and V-7 were 3.4 and 3.9 years old respectively when the biopsy was taken. [22,23] The BMDD results of multiple biopsy samples from one same patient were averaged and thus treated as a single sample.

Informed consent was obtained in each instance from the subject and/or a legal guardian, as appropriate. The study protocol was approved by the Ethics Committee of the Shriners Hospital.

Quantitative Backscattered Electron Imaging (qBEI) analyses

The distal half of femoral bone and transiliac bone biopsy samples were fixed in 70% ethanol, dehydrated in ethanol, and embedded in polymethylmethacrylate. Sample blocks were trimmed using a low speed diamond saw (Isomet-R, Buehler Ltd. Lake Buff, IL, USA). Sectioned bone surfaces were sequentially ground with sand paper with increasing grid number followed by polishing with diamond grains (size down to 0.25 microns) on hard polishing clothes by a PM5 Logitech instrument (Glasgow, Scotland). Finally the sample surface was carbon coated by vacuum evaporation (SCD 004 Balzers, Lichtenstein).

The qBEI technique is well established and validated and the details of the method have been published elsewhere [24]. Briefly, qBEI makes use of the fact that the intensity of electrons backscattered from a depth of 1.5 microns from the surface-layer of a sectioned bone area is proportional to the weight concentration of mineral (hydroxyapatite) and thus calcium in bone. A digital electron microscope (DSM 962, Zeiss, Oberkochen, Germany) equipped with a four quadrant semiconductor backscattered electron BE detector was used. The BE-signal (gray scale) was calibrated using the “atomic number contrast” between carbon (C, Z=6) and aluminum (Al, Z=13) as reference materials. Carbon was set to gray level index 25 and Al to

225, respectively. This allows a scaling also into weight % (wt%) Ca, whereby, osteoid (Z~6) has 0 wt% Ca and pure hydroxyapatite (Z=14.06) has 39.86 wt% Ca according to its composition. Thus, one gray level step corresponds to 0.17 wt% Ca as a consequence of this calibration protocol.

Digital calibrated BE-images with a 200x (resolution 1 microns/pixel) and a 50x (resolution 4 microns/pixel) nominal magnification for the femoral mouse bone and for the transiliac bone samples, respectively were acquired, reflecting the spatial distribution of Ca-content. From these images, gray-level histograms (frequency distributions) were generated indicating the percentage of mineralized bone area (*y* axis) corresponding to the number of pixels with a certain gray level (*x* axis). Following calibration, the BE-image gray-level distribution can be interpreted as a wt% Ca bone mineralization density distribution (BMDD) for bone tissue or as mineralization density distribution for mineralized tissue in general.

The following BMDD parameters were calculated (Fig.1) [25] in both murine and human sample sets: 1) CaMean is the weighted average Ca concentration of the mineralized tissue area, obtained from the integrated area under the BMDD curve. 2) CaPeak is the peak position of the BMDD histogram showing the most frequently occurring wt% Ca of the measured areas. 3) CaWidth is the width at half-maximum of the BMDD histogram curve indicating the heterogeneity of mineralization either caused by the co-existence of differently mineralized bone and calcified cartilage matrices and/or similar matrices, but of different ages and therefore different degree of mineralization. 4) CaLow is the amount of low mineralized tissue areas below the 5^{th} percentile of the adult reference BMDD (17.68 wt% Ca). A fifth parameter, CaHigh, was only evaluated in the human bone samples. It refers to the amount of highly mineralized bone tissue, above the 95^{th} percentile of the adult reference BMDD (25.30 wt% Ca). In the distal murine femoral bone, BMDD-parameters were determined separately in the metaphyseal and epiphyseal spongiosa, and in the midshaft cortical region. In the transiliac biopsy samples, cancellous and cortical compartments were evaluated separately.

Statistics

Statistical analysis was performed using SigmaStat for Windows Version 2.03 (SPSS Inc.). Normality of the data was tested by Kolmogorov-Smirnov test. Normally distributed data are given by mean (SD), non-normally distributed data by median [25^{th} percentile; 75^{th} percentile] in the tables. Data from the murine bone samples were tested for differences by t-test (if data were normally distributed) or by Mann-Whitney rank sums tests (if data were not normally distributed). Differences in trabecular or cortical BMDD in OI-VII children versus the young reference population [26] were tested using rank sum tests. Differences of cancellous BMDDs among the OI-types (I, III, IV) from [18,19] and VII were analysed by ANOVA on ranks followed by Dunn´s pairwise comparison. For all analyses, $p<0.05$ was considered significantly different.

Results

Bone mineralization density distribution (BMDD) in mice

BMDD analyses of the distal femur showed different mineral content in different bone locations for both *Crtap*−/− mutant and control mice. CaMean and CaPeak were higher in epiphyseal than in metaphyseal bone, and highest in the cortical midshaft in both genotypes. The heterogeneity of mineralization (CaWidth) and the fraction of low mineralized bone matrix (CaLow) showed the opposite trend and were highest in metaphyseal bone and lowest in the cortical midshaft (Table 1, Fig. 2).

The quantitative comparison of BMDD-parameters between the two genotypes revealed that in all bone locations CaMean (+3.2 % to +3.4 %, P<0.01 to P<0.001) as well as CaPeak (+3.5 % to +6.4 %, P<0.001) were significantly increased in *Crtap*−/− as compared to *Crtap*+/+ mice (see Table 1, Fig.2), while the mineralization of the bone matrix in the *Crtap*−/− mice appeared less heterogeneous (CaWidth −13.3% to −7.8 %, P<0.01 to P<0.001). However, the portion of low mineralized bone, CaLow, was not significantly different between the two genotypes (Fig. 2, Table 1).

BMDD in children with OI type VII

Fig. 3 shows typical results obtained from an iliac biopsy sample (Fig. 3A) of a child with OI type VII (aged 4.2 years). BMDD was shifted distinctly towards higher mineralization compared to the reference BMDD peak of the young reference cohort (n=54) (Fig 3D) [26]. Cortical bone was more heterogeneously mineralized than cancellous bone (cortical CaWidth was larger than cancellous CaWidth). The BE-image of the biopsy sample cortex (Fig. 3B) clearly shows two discrete areas with different mineral content: the periosteal bone matrix was more highly mineralized with a higher density of osteocyte lacunae compared to the endocortical side. This characteristic variation in the cortical compartment is also quantitatively demonstrated by a line profile of Ca-content across the cortical area (Fig. 3C). For comparison, a line profile taken at an analogous external cortex area from a control individual (shown previously [26]) is displayed in light grey. The levels of Ca-content in both cortical regions are higher in the OI type VII sample than in control.

The BMDD-parameters from the 4 cases of children with OI type VII revealed a remarkable overall increase in matrix mineralization density compared to the young reference cohort [26] (Table 2,Fig. 3): In cancellous bone: CaMean +3.3%, p<0.05, CaPeak +3.7% p<0.01 and CaHigh 2.1 to 3.7 times increased (Table 2a); In cortical bone: CaMean +6.2%, p<0.01, CaPeak +7.6% p<0.01, and CaHigh 7.6 to 25.5 times increased. In contrast, the BMDD parameters CaWidth and CaLow were found similar in patients with OI-VII and in the young reference group [26] (Table 2b).

We further compared the BMDD parameter values of cancellous bone of OI type VII with previously published data of OI type I [19], type III and type IV [18]. No significant differences in CaMean, CaWidth, CaLow and CaHigh were found, except CaPeak was lower in OI type VII than in OI type I: - 4.1% p<0.05 (Table 2a).

Discussion

In the present study, we address the effects of CRTAP deficiency on bone material and show that in *Crtap*−/− mice as well as in affected patients with residual CRTAP function, the mineral content of the bone matrix is abnormally high. We found increased mineral densities at all measured sites for both murine femora and human transiliac biopsy samples compared to control animals and to the young reference population [26], respectively. Such an increase in mineralization density was also found previously in the *oim* mouse model [15–17] and in patients with OI type I type III and type IV (with quantitative as well as qualitative type I collagen mutations) [13,14,18,19]. Hence, our data suggest that the complete or almost complete loss of function of the P3H1/CRTAP/CYPB complex lead to a bone feature similar to “classical” OI.

In the murine samples, independently of the genotype, there was a gradual shift towards higher mineralization density (CaMean and CaPeak) from metaphyseal to epiphyseal and cortical diaphyseal bone, reflecting the differences in local tissue age (duration of secondary mineralization). From this observation, it can be deduced that the metaphyseal spongiosa had on average “younger” (more recently formed) bone packets compared to the epiphyseal bone,

though its ossification center was formed later, and to cortical bone of the diaphysis, which had the relative “older” tissue. The gradual decrease of remodeling/modeling activities is also mirrored by the gradual decrease in heterogeneity of bone matrix mineralization (CaWidth) and in the portion of newly formed bone matrix (CaLow) from metaphyseal to epiphseal and cortical diaphyseal bone.

Interestingly, in the *Crtap*−/− mice, the mineral content was increased compared to *Crtap*+/+ mice in each of these bone compartments. Such an increase in mineral content was also found in both cancellous and cortical transiliac bone in the OI-VII patients suggesting a common intrinsic mechanism leading to a higher bone matrix mineralization independently of the local bone turnover rate. According to a recently established computed modeling of the BMDD, an increase in the mean degree of mineralization could in principle indicate either a decrease of bone turnover or an alteration in mineralization kinetics [27,28]. However, surface-based parameters of bone remodeling were normal in the *Crtap*−/− mice [5] and increased in patients [22] and therefore the increase in CaMean and CaPeak rather point towards the altered mineralization kinetics hypothesis. This is consistent with the observation of a modified profile of non-collagenous proteins in OI, which could lead to a loss of control over crystal nucleation and growth [29–31]. Histomorphometric findings have shown that the amount of matrix produced by a single osteoblast is significantly decreased in OI. Indeed, a diminished performance of the individual osteoblast was found in the *Crtap*−/− animals, as well as in the hypomorphic OI type VII patients and in patients with “classical” OI [5,9,22,32]. A fundamental osteoblastic dysfunction in OI, leading to a reduced production of organic matrix combined with a disturbed synthesis of non-collagenous proteins [29–31,33] has been previously correlated with the increased mineralization density and is also consistent with the findings in CRTAP-deficient bone. Two possible mechanisms might contribute to such an increase in matrix mineral density: first, a higher volume fraction of water is available for replacement by mineral due to the altered structure of the collagen itself or to the abnormal posttranslational modifications of the type I collagen heterotrimer [14,34]. Second, the control of mineral nucleation is disturbed due to the abnormal stoichiometry of non-collagenous proteins [19]. In the *oim* mouse, as well as in OI patients, mineral crystal size was found reduced, suggesting a denser packing of the crystals within the bone matrix [11,15,34]. It is also known that a new bone matrix gets mineralized by a rapid increase in mineral content (primary mineralization) followed by a slower one (secondary mineralization) [35–38]. Assuming that the density of nucleation centers is increased for some reason, as might be hypothesized for both the *Crtap*−/− mice and OI patients in general, the mineralization process would be accelerated due to the simultaneous growth of more crystals leading to an increased primary and consequently increased secondary matrix mineralization. Such a model would not only be consistent with the observation that the osteoid produced by *Crtap*−/− osteoblasts is mineralized in an abnormally fast manner [5] but also with the increased CaMean and CaPeak, as well as with the decreased CaWidth of the bone matrix found in the *Crtap*−/− animals. It should be noted that in the OI VII patients studied here there was no significant decrease in CaWidth compared to control references and this may be due to the residual CRTAP expression. Also CaWidth was not always decreased in “classical” OI with collagen gene mutations (Table 2a) [18].

A much higher portion of highly mineralized bone (CaHigh) was found in cancellous and cortical bone of our OI type VII patients compared to the control reference. It should be mentioned that the CaHigh parameter was derived from adult human bone and corresponds to the amount of fully mineralized mature lamellar bone matrix, which in principle needs years to reach this plateau level in mineralization. Consistently, CaHigh was found to be much lower in children compared to adults due to high remodeling activity during growth [39,40]. Thus, even small changes in BMDD towards higher mineralization can generate comparably large increases in this parameter, because of the low reference level. The increase in CaHigh in the

OI type VII patients is not only consistent with the general shift to a higher degree of mineralization but further indicates that the relative amount of primary bone is increased particularly in the cortices, which is in line with previous observations in other types of OI [13]. In the BE-images of transiliac bone samples, primary bone is seen typically as periosteal bone apposition and differs clearly from secondary/remodeled bone by its structure and higher mineral content (Fig. 4 and [14,26]). Primary bone is formed during growth in the cortices to allow rapid lateral expansion and consequently growth of the ilium in young healthy children [39,40].

It is remarkable that the BMDD parameter values of cancellous bone of OI type VII when compared to those previously published on OI type I [19], type III and type IV [18] were not significantly different in CaMean, CaWidth, CaLow and CaHigh, except CaPeak, which was slightly lower in OI type VII than in OI type I. This finding supports a ubiquitous underlying mechanism of increase in matrix mineralization in all these diseases of different etiology. However, the significance of our comparison is limited due to the small amount of samples, especially in the case of the OI type VII patients. Moreover, it remains unclear to what extent the residual CRTAP expression influences the increase of matrix mineral content in our OI VII cohort of patients (e.g. CaPeak).

In conclusion the BMDD data show that CRTAP deficiency results in a shift towards higher mineral content of the bone matrix and therefore in a feature similar to classical OI with collagen gene mutations. An altered mineralization process seems to be responsible for this overall ultimately elevated tissue mineralization density. Further, in our OI type VII patients the increased portion of primary bone is likely reflecting a disturbed bone development. The overall picture is in agreement with the concept that abnormal matrix assembly and composition lead to higher mineral deposition.

Acknowledgments

We thank G. Dinst, Ph. Messmer, and D. Gabriel for careful sample preparations and qBEI measurements. This study was supported by the AUVA (Research funds of the Austrian workers compensation board), by the WGKK (Viennese sickness insurance funds), by NIH grants AR051459 (R.M.), HD22657 (B.L.), DE01771 (B.L.), the Osteogenesis Imperfecta Foundation (R.M.) and the Bone Disease Program of Texas (R.M.). F.R. is a Chercheur-Boursier Clinicien of the Fonds de la Recherche en Santé du Québec. This study was supported by the Shriners of North America.

References

1. Vranka JA, Sakai LY, Bachinger HP. Prolyl 3-hydroxylase 1, enzyme characterization and identification of a novel family of enzymes. J Biol Chem 2004;279:23615–23621. [PubMed: 15044469]
2. Marini JC, Cabral WA, Barnes AM, Chang W. Components of the collagen prolyl 3-hydroxylation complex are crucial for normal bone development. Cell Cycle 2007;6:1675–1681. [PubMed: 17630507]
3. Myllyharju J, Kivirikko KI. Collagens, modifying enzymes and their mutations in humans, flies and worms. Trends Genet 2004;20:33–43. [PubMed: 14698617]
4. Barnes AM, Chang W, Morello R, Cabral WA, Weis M, Eyre DR, Leikin S, Makareeva E, Kuznetsova N, Uveges TE, Ashok A, Flor AW, Mulvihill JJ, Wilson PL, Sundaram UT, Lee B, Marini JC. Deficiency of cartilage-associated protein in recessive lethal osteogenesis imperfecta. N Engl J Med 2006;355:2757–2764. [PubMed: 17192541]
5. Morello R, Bertin TK, Chen Y, Hicks J, Tonachini L, Monticone M, Castagnola P, Rauch F, Glorieux FH, Vranka J, Bachinger HP, Pace JM, Schwarze U, Byers PH, Weis M, Fernandes RJ, Eyre DR, Yao Z, Boyce BF, Lee B. CRTAP is required for prolyl 3- hydroxylation and mutations cause recessive osteogenesis imperfecta. Cell 2006;127:291–304. [PubMed: 17055431]
6. Cabral WA, Chang W, Barnes AM, Weis M, Scott MA, Leikin S, Makareeva E, Kuznetsova NV, Rosenbaum KN, Tifft CJ, Bulas DI, Kozma C, Smith PA, Eyre DR, Marini JC. Prolyl 3-hydroxylase

1 deficiency causes a recessive metabolic bone disorder resembling lethal/severe osteogenesis imperfecta. Nat Genet 2007;39:359–365. [PubMed: 17277775]

7. Bodian DL, Chan TF, Poon A, Schwarze U, Yang K, Byers PH, Kwok PY, Klein TE. Mutation and polymorphism spectrum in osteogenesis imperfecta type II: implications for genotype-phenotype relationships. Hum Mol Genet 2009;18:463–471. [PubMed: 18996919]
8. Sillence DO, Senn A, Danks DM. Genetic heterogeneity in osteogenesis imperfecta. J Med Genet 1979;16:101–116. [PubMed: 458828]
9. Rauch F, Glorieux FH. Osteogenesis imperfecta. Lancet 2004;363:1377–1385. [PubMed: 15110498]
10. Camacho NP, Landis WJ, Boskey AL. Mineral changes in a mouse model of osteogenesis imperfecta detected by Fourier transform infrared microscopy. Connect Tissue Res 1996;35:259–265. [PubMed: 9084664]
11. Fratzl P, Paris O, Klaushofer K, Landis WJ. Bone mineralization in an osteogenesis imperfecta mouse model studied by small-angle x-ray scattering. J Clin Invest 1996;97:396–402. [PubMed: 8567960]
12. Misof K, Landis WJ, Klaushofer K, Fratzl P. Collagen from the osteogenesis imperfecta mouse model (oim) shows reduced resistance against tensile stress. J Clin Invest 1997;100:40–45. [PubMed: 9202055]
13. Jones SJ, Glorieux FH, Travers R, Boyde A. The microscopic structure of bone in normal children and patients with osteogenesis imperfecta: a survey using backscattered electron imaging. Calcif Tissue Int 1999;64:8–17. [PubMed: 9868277]
14. Boyde A, Travers R, Glorieux FH, Jones SJ. The mineralization density of iliac crest bone from children with osteogenesis imperfecta. Calcif Tissue Int 1999;64:185–190. [PubMed: 10024373]
15. Grabner B, Landis WJ, Roschger P, Rinnerthaler S, Peterlik H, Klaushofer K, Fratzl P. Age- and genotype-dependence of bone material properties in the osteogenesis imperfecta murine model (oim). Bone 2001;29:453–457. [PubMed: 11704498]
16. Misof BM, Roschger P, Baldini T, Raggio CL, Zraick V, Root L, Boskey AL, Klaushofer K, Fratzl P, Camacho NP. Differential effects of alendronate treatment on bone from growing osteogenesis imperfecta and wild-type mouse. Bone 2005;36:150–158. [PubMed: 15664013]
17. Carleton SM, McBride DJ, Carson WL, Huntington CE, Twenter KL, Rolwes KM, Winkelmann CT, Morris JS, Taylor JF, Phillips CL. Role of genetic background in determining phenotypic severity throughout postnatal development and at peak bone mass in Col1a2 deficient mice (oim). Bone 2008;42:681–694. [PubMed: 18313376]
18. Weber M, Roschger P, Fratzl-Zelman N, Schoberl T, Rauch F, Glorieux FH, Fratzl P, Klaushofer K. Pamidronate does not adversely affect bone intrinsic material properties in children with osteogenesis imperfecta. Bone 2006;39:616–622. [PubMed: 16644299]
19. Roschger P, Fratzl-Zelman N, Misof BM, Glorieux FH, Klaushofer K, Rauch F. Evidence that abnormal high bone mineralization in growing children with osteogenesis imperfecta is not associated with specific collagen mutations. Calcif Tissue Int 2008;82:263–270. [PubMed: 18311573]
20. Glorieux FH, Rauch F, Plotkin H, Ward L, Travers R, Roughley P, Lalic L, Glorieux DF, Fassier F, Bishop NJ. Type V osteogenesis imperfecta: a new form of brittle bone disease. J Bone Miner Res 2000;15:1650–1658. [PubMed: 10976985]
21. Glorieux FH, Ward LM, Rauch F, Lalic L, Roughley PJ, Travers R. Osteogenesis imperfecta type VI: a form of brittle bone disease with a mineralization defect. J Bone Miner Res 2002;17:30–38. [PubMed: 11771667]
22. Ward LM, Rauch F, Travers R, Chabot G, Azouz EM, Lalic L, Roughley PJ, Glorieux FH. Osteogenesis imperfecta type VII: an autosomal recessive form of brittle bone disease. Bone 2002;31:12–18. [PubMed: 12110406]
23. Cheung MS, Glorieux FH, Rauch F. Intravenous Pamidronate in Osteogenesis Imperfecta Type VII. Calcif Tissue Int. 2009
24. Roschger P, Fratzl P, Eschberger J, Klaushofer K. Validation of quantitative backscattered electron imaging for the measurement of mineral density distribution in human bone biopsies. Bone 1998;23:319–326. [PubMed: 9763143]
25. Roschger P, Paschalis EP, Fratzl P, Klaushofer K. Bone mineralization density distribution in health and disease. Bone 2008;42:456–466. [PubMed: 18096457]

26. Fratzl-Zelman N, Roschger P, Misof BM, Pfeffer S, Glorieux FH, Klaushofer K, Rauch F. Normative data on mineralization density distribution in iliac bone biopsies of children, adolescents and young adults. Bone 2009;44:1043–1048. [PubMed: 19268565]
27. Ruffoni D, Fratzl P, Roschger P, Klaushofer K, Weinkamer R. The bone mineralization density distribution as a fingerprint of the mineralization process. Bone 2007;40:1308–1319. [PubMed: 17337263]
28. Ruffoni D, Fratzl P, Roschger P, Phipps R, Klaushofer K, Weinkamer R. Effect of temporal changes in bone turnover on the bone mineralization density distribution: a computer simulation study. J Bone Miner Res 2008;23:1905–1914. [PubMed: 18665790]
29. Vetter U, Fisher LW, Mintz KP, Kopp JB, Tuross N, Termine JD, Robey PG. Osteogenesis imperfecta: changes in noncollagenous proteins in bone. J Bone Miner Res 1991;6:501–505. [PubMed: 2068957]
30. Fedarko NS, Robey PG, Vetter UK. Extracellular matrix stoichiometry in osteoblasts from patients with osteogenesis imperfecta. J Bone Miner Res 1995;10:1122–1129. [PubMed: 7484289]
31. Fedarko NS, Vetter U, Robey PG. The bone cell biology of osteogenesis imperfecta. Connect Tissue Res 1995;31:269–273. [PubMed: 15612366]
32. Rauch F, Travers R, Parfitt AM, Glorieux FH. Static and dynamic bone histomorphometry in children with osteogenesis imperfecta. Bone 2000;26:581–589. [PubMed: 10831929]
33. Grzesik WJ, Frazier CR, Shapiro JR, Sponseller PD, Robey PG, Fedarko NS. Age-related changes in human bone proteoglycan structure. Impact of osteogenesis imperfecta. J Biol Chem 2002;277:43638–43647. [PubMed: 12221073]
34. Traub W, Arad T, Vetter U, Weiner S. Ultrastructural studies of bones from patients with osteogenesis imperfecta. Matrix Biol 1994;14:337–345. [PubMed: 7827757]
35. Roschger P, Grabner BM, Rinnerthaler S, Tesch W, Kneissel M, Berzlanovich A, Klaushofer K, Fratzl P. Structural development of the mineralized tissue in the human L4 vertebral body. J Struct Biol 2001;136:126–136. [PubMed: 11886214]
36. Boivin G, Meunier PJ. Changes in bone remodeling rate influence the degree of mineralization of bone. Connect Tissue Res 2002;43:535–537. [PubMed: 12489211]
37. Boivin G, Meunier PJ. Methodological considerations in measurement of bone mineral content. Osteoporos Int 2003;14:S22–S27. discussion S27–8. [PubMed: 14504702]
38. Misof BM, Roschger P, Cosman F, Kurland ES, Tesch W, Messmer P, Dempster DW, Nieves J, Shane E, Fratzl P, Klaushofer K, Bilezikian J, Lindsay R. Effects of intermittent parathyroid hormone administration on bone mineralization density in iliac crest biopsies from patients with osteoporosis: a paired study before and after treatment. J Clin Endocrinol Metab 2003;88:1150–1156. [PubMed: 12629098]
39. Rauch F, Travers R, Glorieux FH. Cellular activity on the seven surfaces of iliac bone: a histomorphometric study in children and adolescents. J Bone Miner Res 2006;21:513–519. [PubMed: 16598370]
40. Parfitt AM, Travers R, Rauch F, Glorieux FH. Structural and cellular changes during bone growth in healthy children. Bone 2000;27:487–494. [PubMed: 11033443]
41. Fratzl P, Fratzl-Zelman N, Klaushofer K. Collagen packing and mineralization. An x-ray scattering investigation of turkey leg tendon. Biophys J 1993;64:260–266. [PubMed: 8431546]

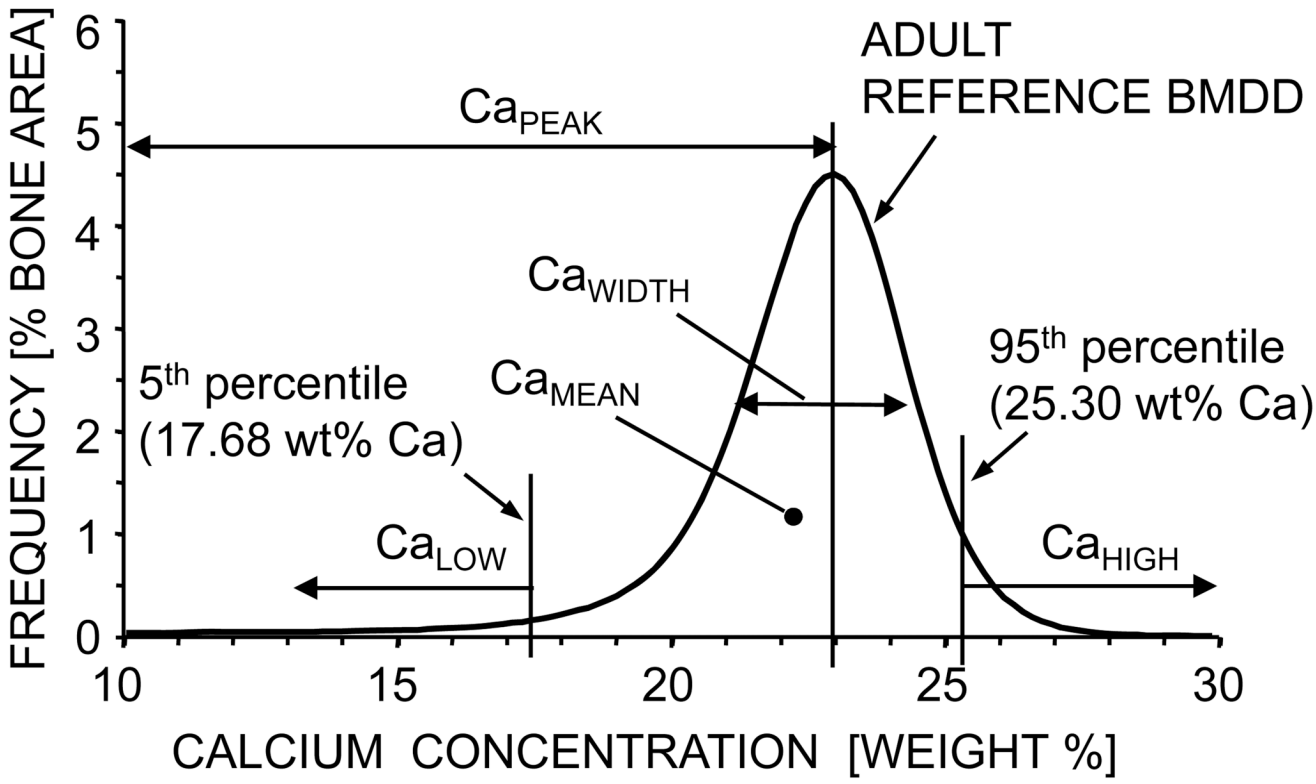

Figure 1.
Definition of the BMDD-parameters: All BMDD parameters used in this article (CaMean, CaPeak, CaWidth, CaLow, CaHigh) are derived from the BMDD curve as illustrated. Note that the cut off value for CaLow (17.68 wt% Ca) and CaHigh (25.30 wt% Ca) are derived from the reference BMDD of normal human adult trabecular bone [25]. All BMDD curves in this article are shown in a way that the individual histogram data points (frequency of Ca-content) are connected by a line without showing the data point itself, thus sometimes the BMDD curve can have a hand-drawn character (Fig. 2 and Fig. 3).

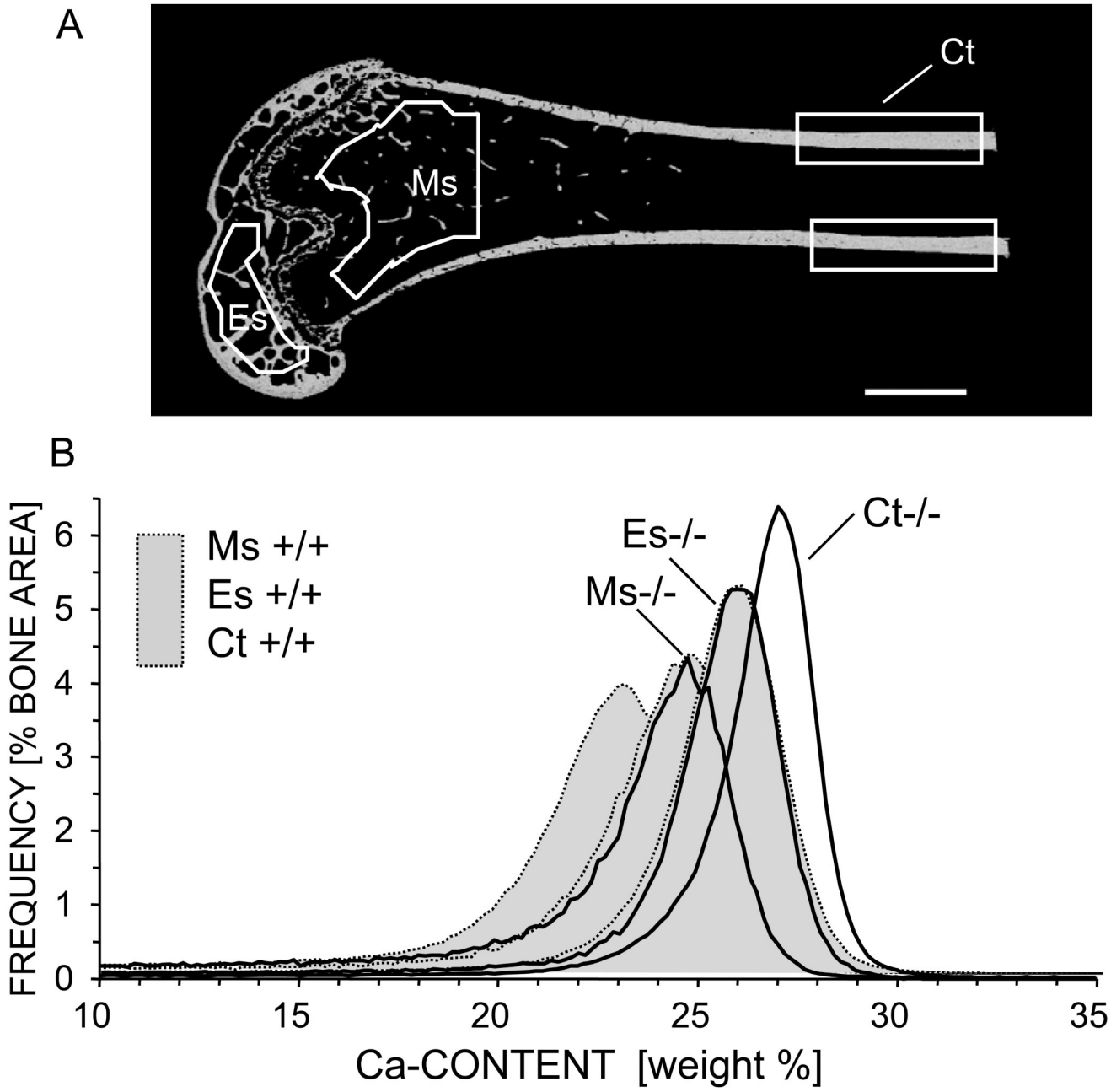

Figure 2.
BMDD measurements of distal femur from *Crtap*−/− and *Crtap*+/+ mice: A) BE-image of a *Crtap*−/− femur (longitudinal section) showing the three regions of interest in which BMDD analysis were performed: Ms = cancellous metaphyseal bone, Es = cancellous epiphyseal bone, Ct = cortical midshaft bone. B) Corresponding BMDD curves for each ROI: solid black line shows *Crtap*−/− and light grey filled curves (dotted line) represents a *Crtap*+/+ mouse. Scale bar represent 1mm.

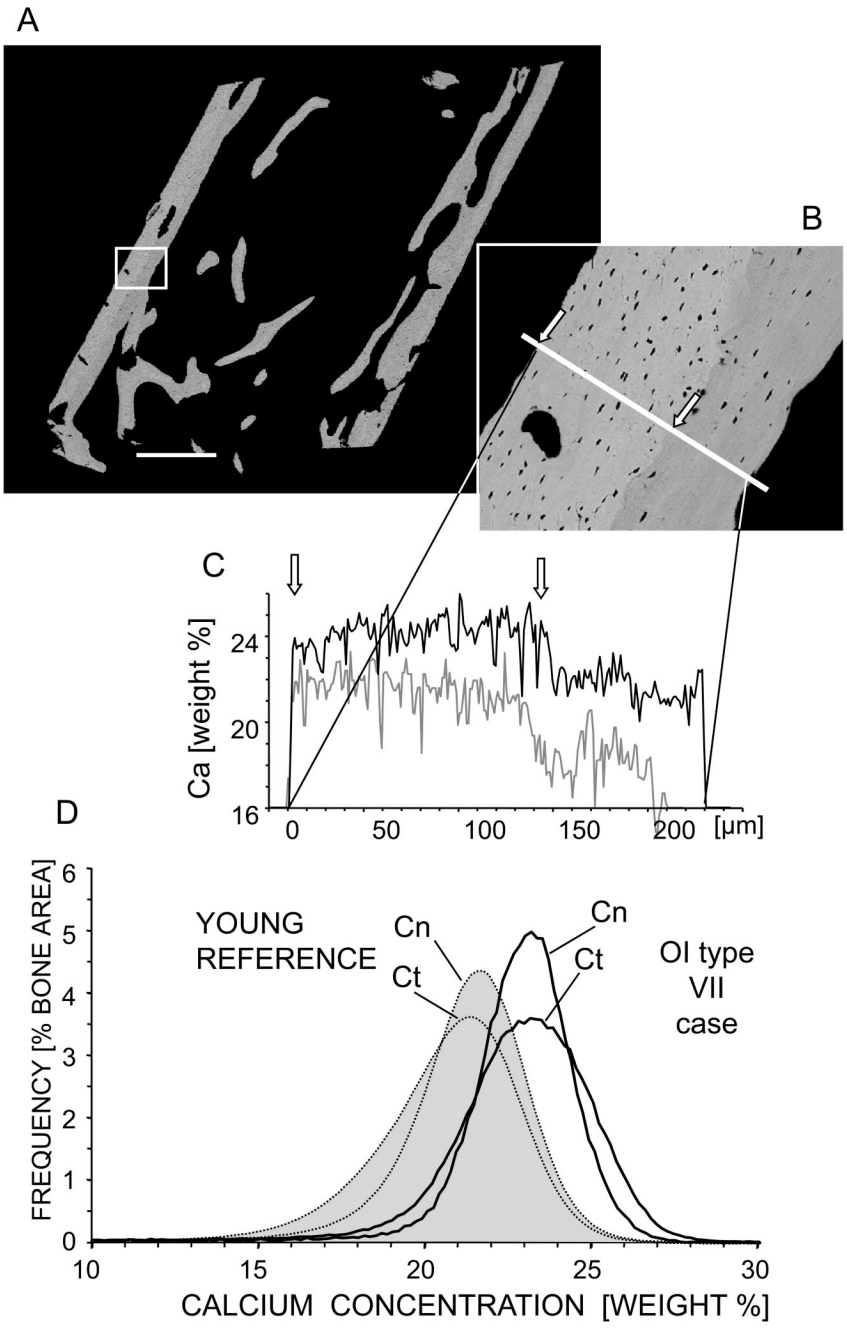

Figure 3.

BMDD analysis of a 4.2 old OI type VII patient. A) BE-image overview of the entire biopsy sample showing. Scale bar indicates 1 mm. B) Zoomed in detail of cortical bone region showing periosteal primary highly mineralized bone (between the arrows) and lower mineralized endocortical bone. C) Corresponding Ca-content profile along the line marked through the cortex in (B): Black solid line = OI type VII patient; Gray solid line = example of analogous region of young controls previously published [26]. D) Corresponding BMDD curves: Black solid line represents OI type VII patient; Light gray filled curves (dotted line) represent YOUNG REFERENCE (n=54) [26]. Cn = cancellous and Ct = cortical bone. Scale bar represent 1mm.

Table 1

BMDD parameters of cancellous metaphysis (MS Cn), epiphysis (ES Cn) and cortical diaphysis (D Ct) in the *Crtap*−/− mice compared to the *Crtap*+/+ animals.

	***Crtap*+/+ MS Cn (n=15)**	***Crtap*−/− MS Cn (n=12)**
CaMean [wt% Ca]	22.50 (0.74)	23.26** (0.47)
CaPeak [wt% Ca]	23.83 (0.62)	24.93*** (0.40)
CaWidth [Δwt% Ca]	3.64 [3.47;3.99]	3.21** [2.95;3.64]
CaLow [%]	8.85 (2.19)	10.05 (1.82)
	Crtap+/+ ES Cn (n=15)	*Crtap*−/− ES Cn (n=12)
CaMean [wt% Ca]	23.71 [23.38; 24.02]	24.47*** [24.10; 24.98]
CaPeak [wt% Ca]	24.21 (0.56)	25.75*** (0.63)
CaWidth [Δwt% Ca]	3.06 (0.21)	2.82* (0.34)
CaLow [%]	5.29 (0.99)	5.87 (1.19)
	Crtap+/+ D Ct (n=15)	*Crtap* −/− D Ct (n=12)
CaMean [wt% Ca]	25.61 (0.44)	26.42*** 0.43
CaPeak [wt% Ca]	26.20 (0.44)	27.12*** (0.33)
CaWidth [Δwt% Ca]	2.92 (0.13)	2.53*** (0.12)
CaLow [%]	2.01 [1.87; 2.23]	2.11 [1.80; 2.38]

Data shown are mean (SD) or median [25%; 75%] for *Crtap*+/+ and *Crtap*−/− mice

*, **, *** significant difference ($p<0.05$, $p<0.01$, $p<0.001$, respectively) of BMDD results between *Crtap*+/+ and *Crtap*−/− mice.

Table 2

a: Comparison of cancellous BMDD parameters of the OI type VII study group with the young reference population [26] and comparison of the BMDD parameters among different OI-groups: OI type VII with previously published OI type I [19], OI type III and OI type IV [18]					
	Young Reference n=54	**OI type VII n=4**	**OI type I n=19**	**OI type III n=3**	**OI type IV n=8**
CaMean [wt% Ca]	20.95 (0.57)	21.65 * [21.48; 21.75]	22.43 (0.63)	22.49 [22.38; 23.06]	22.61 (0.74)
CaPeak [wt% Ca]	21.66 (0.52)	22.43 ** [22.30; 22.49]	23.39*a* (0.57)	22.88 [22.88; 23.53]	23.24 (0.68)
CaWidth [Δwt% Ca]	3.47 [3.12; 3.64]	3.21 [3.04; 3.29]	3.08 (0.28)	3.29 [3.03; 3.42]	3.53 *b* (0.29)
CaLow [%]	6.14 [4.95; 7.99]	6.04 [5.72; 6.46]	5.94 (2.05)	3.90 [3.64; 3.97]	4.30 (1.75)
CaHigh [%]	0.90 [0.44; 1.47]	2.52 ** [1.96; 3.20]	7.54 [5.00; 11.82]	4.95 [4.24; 11.86]	6.99 [3.13; 9.61]

b: Comparison of cortical BMDD parameters of the OI type VII study group with young reference population [26]		
	Young Reference (n=53)	**OI type VII (n=4)**
CaMean [wt% Ca]	20.45 [19.68; 21.04]	21.72** [21.71; 21.87]
CaPeak [wt% Ca]	21.14 [20.62; 21.75]	22.75** [22.40; 23.11]
CaWidth [Δwt% Ca]	3.81 [3.38; 4.38]	4.10 [3.64; 4.57]
CaLow [%]	9.06 [6.22; 15.00]	6.01 [5.41; 7.87]
CaHigh [%]	0.46 [0.28; 1.22]	8.11*** [4.83; 11.14]

Data are mean (SD) or median [25th percentile; 75th percentile]

** p<0.01,

* p<0.05 comparison of OI type VII to normal reference data (rank sum test)

a Comparison among the OI-types: ANOVA on ranks: p<0.05 versus OI type VII,

b p<0.05 versus OI type I (Dunn's posthoc test)

*** $p<0.001$,

** $p<0.01$, comparison to normal reference data (rank sum test)